Pressure Dependence of Mn^{2+} Luminescence in Differently Sized ZnS:Mn Nanoparticles

F. H. Su, Z. L. Fang, B. S. Ma, K. Ding, and G. H. Li*

National Laboratory for Superlattices and Microstructures, Institute of Semiconductors, Chinese Academy of Sciences, P.O. Box 912, Beijing 100083, China

W. Chen*

Nomadics, Inc., 1024 South Innovation Way, Stillwater, Oklahoma 74074

Received: December 30, 2002; In Final Form: May 12, 2003

The pressure behavior of Mn^{2+} emission in the 10-, 4.5-, 3.5-, 3-, and 1-nm-sized ZnS:Mn^{2+} nanoparticles is investigated. The emission shifts to lower energies with increasing pressure, and the shift rate (the absolute value of the pressure coefficient) is larger in the ZnS:Mn^{2+} nanoparticles than in bulk. The pressure coefficient increases with the decrease in particle size with the 1-nm-sized particles as an exception. Pressure coefficient calculations based on the crystal field theory are in agreement with the experimental results. The pressure dependence of the emission intensity is also size dependent. For nanoparticles 1 and 3 nm in size, the luminescence intensity of Mn^{2+} decreases dramatically with increasing pressure, while, for bulk and particles with average sizes of 3.5, 4.5, and 10 nm, the luminescence intensity of Mn^{2+} is virtually unchanged at different pressures. The bandwidth increases faster with increasing pressure for smaller particles. This is perhaps due to the fact that there are more Mn^{2+} ions at the near-surface sites and because the phonon frequency is greater for smaller particles. These new phenomena provide some insight into the luminescence behavior of Mn^{2+} in ZnS:Mn^{2+} nanoparticles.

Introduction

Semiconductor nanocrystals have attracted much attention in recent years. Due to the quantum confinement effect, semiconductor nanocrystals exhibit some unique optical properties such as a blue shift in emission with decreasing size.[1] In 1994, Bhargava et al. reported the luminescence enhancement and the shortening of the decay lifetime of Mn^{2+}-related emissions in ZnS nanoparticles.[2] However, the shortening of the decay lifetime was found to be a misinterpretation.[3−6] Recently, a submicrosecond ultrafast component was observed in both bulk and CdMnTe quantum dots, which it is attributed to an efficient spin cross-relaxation between localized spins of Mn^{2+} ions and spins of free carriers.[7] Hot luminescence was also reported in ZnS:Mn^{2+} nanoparticles,[8] but it was pointed out that the hot luminescence could be due to an artifact.[9] Bhargava et al. suggested that the hybridization of the s−p electron orbital of the ZnS host and the d electron orbital of the Mn^{2+} ion accounts for the lifetime shortening and the luminescence enhancement,[2] whereas there is no strong evidence for the hybridization of the s−p electron orbital of the ZnS host and d electron orbital of Mn^{2+} ions. These conflicting results indicate that the luminescence mechanism in ZnS:Mn^{2+} nanoparticles is not clear yet and awaits further investigation.

Variation of hydrostatic pressure can change the interatomic distance and the overlap among adjacent electronic orbitals. Pressure dependence of luminescence can provide useful information about the electronic state of an emitter and the interaction between the luminescence centers and their hosts. It has been reported that the pressure behavior of a 4.5-nm-sized ZnS:Mn^{2+} nanoparticle is not much different from that of the bulk.[10] To our knowledge, there has been no work done on the pressure dependence of luminescence in ZnS:Mn nanoparticles with different sizes. In this paper, we present the pressure behaviors of photoluminescence for ZnS:Mn^{2+} nanocrystals of different sizes compared to the bulk. The pressure dependence of Mn^{2+} luminescence in ZnS:Mn^{2+} nanoparticles, both in emission energy and intensity, is actually size dependent, and the behavior can be reasonably illustrated on the basis of crystal field theory and the quantum confinement effect.

Samples and Experiments

The average sizes of the particles, estimated from high-resolution transmission electron microscopy (HRTEM) and X-ray diffraction (XRD), are approximately 1, 3, 3.5, 4.5, and 10 nm, respectively.[11] The 10-nm-sized particles were naked without any capping, while the 3- and 4.5-nm-sized particles were capped with methacrylic acid and the 3.5-nm-sized particles were capped with methacrylic acid and citric acid. On the other hand, the nanoparticles of 1 nm were formed in cavities of ultrastable zeolite-Y (USY) by solid-state diffusion at high temperature.[11] Details about the preparation and structure of the samples have been reported previously.[11,12] A commercial bulk ZnS:Mn sample was also measured for comparison.

The photoluminescence (PL) measurements under hydrostatic pressure were performed in a gasketed diamond-anvil cell (DAC) at room temperature. Some powder samples, together with a piece of ruby chip, were placed in a stainless steel gasket with a hole 300 μm in diameter. A 4:1 methanol−ethanol mixture was used as the pressure-transmitting medium. The pressure was determined by using the standard ruby-fluorescence technique and could be varied from 0 to 6 GPa. For the

* Corresponding authors. E-mail: ghli@red.semi.ac.cn (G.H.L.); wchen@nomadics.com (W.C.). Phone: 405-372-9535 (W.C.). Fax: 405-372-9537 (W.C.).

10.1021/jp0278566 CCC: $25.00
Published on Web 06/27/2003

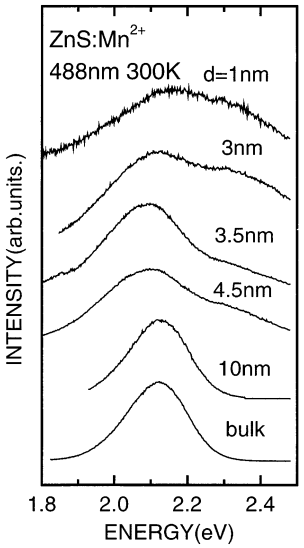

Figure 1. Normalized emission spectra of 1-, 3-, 3.5-, 4.5-, and 10-nm sized ZnS:Mn^{2+} nanoparticles and bulk ZnS:Mn^{2+} measured under atmospheric pressure, respectively.

measurement of emission spectra, the 488-nm line of an Ar^+ ion laser was used as an excitation source. The emitted light was dispersed by a JY-HRD1 double-grating monochromator and detected by a cooled GaAs photomultiplier operating in the photon-counting mode.

Result and Discussion

The emission spectra of ZnS:Mn^{2+} nanoparticles of different sizes and the corresponding bulk sample under atmospheric pressure are displayed in Figure 1. The spectra were measured from outside the DAC and have been normalized. The orange emission under excitation at 488 nm is from the $^4T_1 \rightarrow {}^6A_1$ transition of Mn^{2+} ions in ZnS.[2] The emission energies of bulk and the 10-nm-sized nanoparticles are very close, 2.14 and 2.13 eV, respectively. The emission energies are 2.09, 2.08, and 2.10 eV for the 4.5-, 3.5-, and 3-nm-sized samples, respectively, which are red shifted from that of bulk ZnS:Mn.[2+] The red shift may come from the quantum confinement effect in nanoparticles, which leads to the change of crystal field surrounding Mn^{2+} ions.[11] On the other hand, the 1-nm-sized nanoparticles have a broad emission band centered at approximately 2.2 eV, which is higher than the emission energy of bulk. This is attributed to a weaker electron−phonon coupling and a smaller Stokes shift in these nanoparticles.[11]

The luminescence spectra at different pressures are displayed in Figure 2. The Mn^{2+} emission shifts to lower energy levels with increasing pressure. For the bulk and the particles 10, 4.5, and 3.5 nm in size, the emission intensity is weakly dependent on pressure, while for the 3- and 1-nm nanoparticles the emission intensity of Mn^{2+} decreases prominently with increasing pressure. This can be seen from Figure 2 and more clearly from Figure 3, in which the pressure dependence of the integrated intensity of the Mn^{2+} emissions is drawn. The decrease in intensity is so fast with increasing pressure for the 1-nm-sized particles that no luminescence is detectable when the pressure is higher than 1.4 GPa. It is noted that the intensities of Mn^{2+} emissions in the 3- and 1-nm-sized particles are weaker than those of other samples under 488-nm excitation at atmospheric pressure.

Chen et al.[11] have reported luminescence enhancement in an identical sample with 1-nm-sized particles under 260-nm excitation. This is an indirect excitation—i.e., excitation into

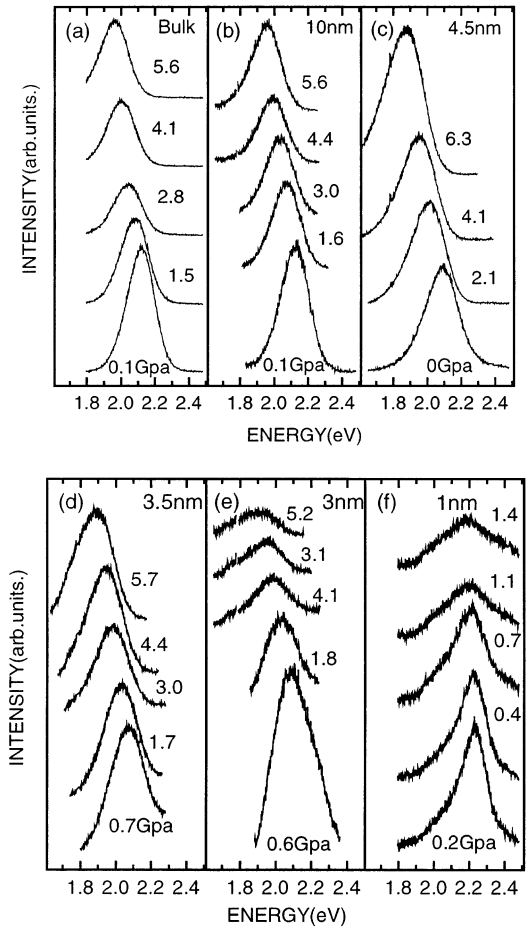

Figure 2. Emission spectra of bulk and 1-, 3-, 3.5-, 4.5-, and 10-nm sized ZnS:Mn^{2+} nanoparticles measured at different pressures, respectively.

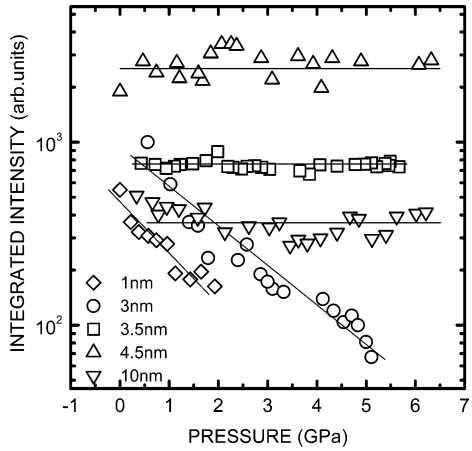

Figure 3. Pressure dependence of the integrated intensity of the orange emission for 1-, 3-, 3.5-, 4.5-, and 10-nm-sized ZnS:Mn^{2+} nanoparticles. The solid lines serve only to guide the eye.

the excited levels of the ZnS host followed by an energy transfer from ZnS to Mn^{2+} that produces luminescence. However, in our measurements, the excitation at 488 nm is a direct excitation of Mn^{2+} ions and a different phenomenon is observed. This indicates that the luminescence intensity is closely related to the excitation energy and mechanism.

Figure 4 shows the absorption (ABS) and photoluminescence excitation (PLE) spectra of the 3.5-nm particle sample. The absorption edge is at 335 nm with an absorption peak at 310 nm which is about 30-nm blue-shifted from the absorption of

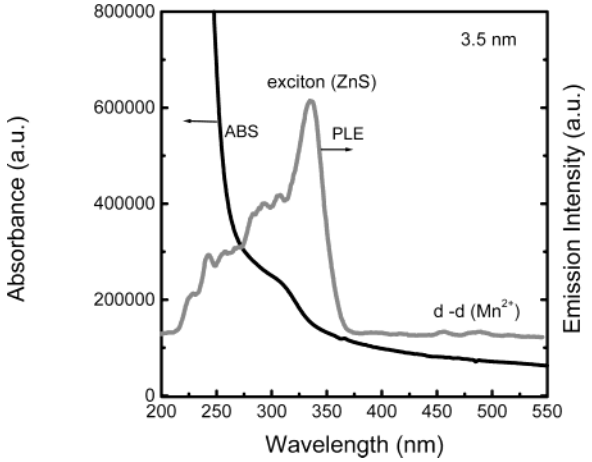

Figure 4. Absorption (ABS) and photoluminescnce excitation (PLE, emission at 581 nm) of the 3.5-nm-sized ZnS:Mn^{2+} nanoparticle sample.

bulk ZnS:Mn^{2+} at 342 nm[5] as a result of quantum size confinement. The absorption peak in the excitation spectrum is at 335 nm, which corresponds to the absorption edge as reported for ZnS nanoparticles.[13] Absorption bands from 375 to 550 nm are from the d−d transitions of Mn^{2+}.[11] The luminescence efficiency for ZnS:Mn^{2+} from indirect excitation is much higher than that from direct excitation because the band-to-band absorption of ZnS is much stronger than the d−d absorption of Mn^{2+}. Thus, in the indirect excitation, the energy transfer from the ZnS host to Mn^{2+} is a dominant process in determining the luminescence efficiency.

For smaller nanoparticles, the absorption coefficient increases due to the increase of the overlap of electron−hole wave functions. Therefore, it is reasonable that the luminescence is enhanced with decreasing size as observed by several groups.[2,11,14] However, for the direct excitation of Mn^{2+}, luminescence efficiency is mainly determined by the emitter transition properties and interaction with its surroundings.[16] For smaller particles, the nonradiative contribution from surface-related defects is larger due to energy or carrier transfer from Mn^{2+} to these defects,[16] and this is perhaps the reason for the weakening of luminescence in smaller particles under direct excitation. The energy transfer to surface-related defects may also be responsible for the rapid luminescence quenching of Mn^{2+} at higher pressures for the 3- and 1-nm nanoparticles. The surface-to-volume ratio (a) is inversely proportional to the diameter (d) of the particle:

$$a \propto \frac{1}{d} \tag{1}$$

The pressure coefficient of the surface-to-volume ratio is

$$\frac{\mathrm{d}a}{\mathrm{d}P} \propto -\frac{1}{\mathrm{d}^2}\frac{\mathrm{d}d}{\mathrm{d}P} = \left(-\frac{1}{d}\frac{\mathrm{d}d}{\mathrm{d}P}\right)\frac{1}{d} \tag{2}$$

Since $V \propto d^3$, thus,

$$-\frac{1}{d}\frac{\mathrm{d}d}{\mathrm{d}P} \propto \frac{1}{3}\left(-\frac{1}{V}\frac{\mathrm{d}V}{\mathrm{d}P}\right) = \frac{1}{3}k \tag{3}$$

Therefore, the pressure dependence of the surface-to-volume ratio of nanoparticle can be expressed as

$$\frac{\mathrm{d}a}{\mathrm{d}P} \propto k\frac{1}{d} \tag{4}$$

where $k = -1/V(\mathrm{d}V/\mathrm{d}P)$ denotes the volume compressibility

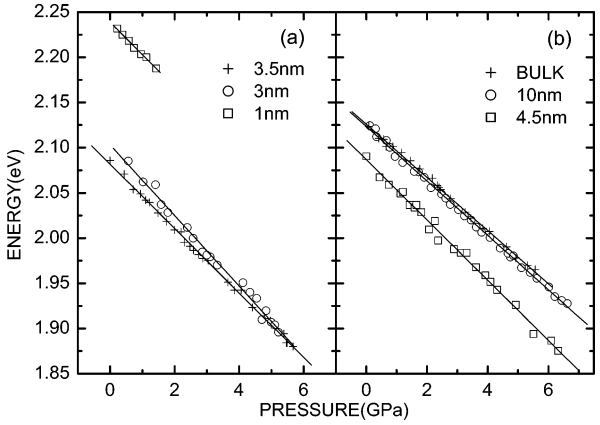

Figure 5. Pressure dependence of the orange emission in ZnS:Mn^{2+} nanoparticles and corresponding bulk. The solid lines are the least-squares fit to the data.

of ZnS. Thus, the pressure-induced change of the surface-to-volume ratio is also size dependent.

For smaller particles, the variation of the surface-to-volume ratio with pressure is larger. This may accelerate the energy transfer from Mn^{2+} ions to the surface-related defects and quenches the luminescence. Moreover, we should point out that for the 1-nm-sized particles formed in zeolite-Y have very well passivated surfaces and the concentration of surface-related defects should be low.[11] However, all Mn^{2+} ions in these particles are distributed in the near-surface sites as determined from electron spin resonance measurements.[11] In this case, the quenching by surface-related defects is still not avoidable. In addition, it was observed that carriers generated in the nanoparticles formed in zeolites may migrate to the defects in the zeolite framework such as oxygen vacancies.[15] This is perhaps another reason for the pressure quenching of the 1-nm-sized particles at high pressures.

The pressure dependence of the PL peak energy for orange emission is shown in Figure 5. The solid lines in Figure 5 represent the result of the least-squares fit to the experimental data using the linear relationship

$$E(P) = E_0 + \alpha P \tag{5}$$

where α is the pressure coefficient and E_0 represents the emission energy at $P = 0$ GPa. The obtained pressure coefficients are listed in Table 1. The absolute values of the pressure coefficients of the nanoparticles are larger than that of the bulk sample. Moreover, the absolute pressure coefficient increases with decreasing particle size with the 1-nm-sized particles as an exception, which is a little smaller than that of the 3-nm-sized sample. As pointed out, the special behavior of the 1-nm-sized particles is probably related to their special environments as they are encapsulated in zeolite.[16] It was also observed that the temperature dependence of its emission energy is similar to that of bulk ZnS:Mn^{2+}, even though most Mn^{2+} ions are at the near-surface sites in the particles formed in zeolite-Y.[15] This is attributed to the fact that surface passivation of the nanoparticles encapsulated in zeolites is actually via chemical bonding between the anions (Zn^{2+}) at the nanoparticle surfaces and the zeolite-framework oxygen ions (O^{2-}).[17] In this case, surrounding Mn^{2+} in ZnS:Mn^{2+} in zeolite is similar to Mn^{2+} in bulk ZnS:Mn^{2+}. This is likely the reason for the sample having luminescence temperature behaviors similar to bulk. Similarly, we believe this is the reason the 1-nm-sized particles have a lower pressure coefficient value (absolute) than that of the 3-nm-sized particles.

TABLE 1: Parameters Obtained from the Least-Squares Fit to the Measured Pressure Shift, Crystal Field Parameter *Dq*, Racah Parameter *B*, and Calculated Pressure Coefficient Based on Crystal Field Theory[a]

diameter (nm)	E_0 (eV)	a (meV/GPa)	B (cm^{-1})	Dq (cm^{-1})	dE/dP (meV/GPa)	(dE/dP)^1 (meV/GPa)	(dE/dP)^2 (meV/GPa)
1	2.239 ± 0.002	-36 ± 2	520	494	-31.6	-13.0	-18.7
3	2.103 ± 0.003	-39 ± 1					
3.5	2.082 ± 0.001	-35.7 ± 0.8	490	512	-33.1	-13.5	-19.7
4.5	2.087 ± 0.002	-33.3 ± 0.6	551	516	-30.9	-13.6	-17.4
10	2.123 ± 0.001	-30.1 ± 0.3	521	519	-31.9	-13.6	-18.3
bulk	2.126 ± 0.001	-29.4 ± 0.3	609	510	-29.1	-13.4	-15.7

[a] See text for more details.

The pressure coefficient of Mn^{2+} emission in ZnS:Mn^{2+} can be calculated by using crystal field theory.[18] According to the crystal field theory, the energy level of Mn^{2+} ions in ZnS:Mn can be expressed as a function of the crystal field parameter Dq and the Racah parameters B and C. The Racah parameters describe the interaction between 3d electrons of Mn^{2+} ion. The Tanabe−Sugano diagram[19] gives normalized energy E/B as a function of the normalized crystal field parameter Dq/B. Therefore, the pressure shift of the peak energy of the orange emission, dE/dP, can be expressed as a function of dDq/dP and dB/dP, assuming that the Racah parameter ratio C/B is independent of the pressure[20]

$$\frac{\mathrm{d}E}{\mathrm{d}P} = \delta\frac{\mathrm{d}Dq}{\mathrm{d}P} + (E_0 - Dq\delta)\frac{1}{B}\frac{\mathrm{d}B}{\mathrm{d}P} \tag{6}$$

where $\delta = \mathrm{d}(E/B)/\mathrm{d}(Dq/B)$ is the slope of the curve E/B vs Dq/B at the value of Dq/B derived from the corresponding transition $^4T_1$ to $^6A_1$ in the Sugano−Tanabe diagram. The value of δ is -10 for the Mn^{2+} ions. E_0 is the PL peak energy of orange emission at $P = 0$ GPa. The parameters Dq, B, and C can be estimated from the following equations:[19,21]

$$22B + 7C = {}^4A_2({}^4F) \tag{7}$$

$$17B + 5C = {}^4E({}^4D) \tag{8}$$

$$10B + 5C = {}^4A_1, {}^4E({}^4G) \tag{9}$$

$$100Dq^2 - (14B + 5C - E_1)(22B + 7C - E_1) = \frac{12B^2(E_1 - 22B - 7C)}{(13B + 5C - E_1)} \tag{10}$$

$$100Dq^2 - (10B + 7C - E_2)(10B + 5C - E_2) = \frac{36B^2(E_2 - 10B - 5C)}{(19B + 7C - E_2)} \tag{11}$$

Here $E_1 = E(^4T_2) - E(^6A_1)$ and $E_2 = E(^4T_1) - E(^6A_1)$. The transition energies $^6A_1 \rightarrow {}^4A_2({}^4F)$, $^6A_1 \rightarrow {}^4E({}^4D)$, $^6A_1 \rightarrow {}^4A_1$, $^4E(^4G)$, E_1, and E_2 have been measured by Chen et al. for the same series of ZnS:Mn^{2+} nanoparticles except for the 3-nm sample from the luminescence excitation spectra.[11] The value of B and C can be calculated from eqs 7−9 directly using the measured transition energies. Dq is then estimated as the average value of the two values obtained from eqs 10 and 11. The estimated values of the parameters Dq and B for differently sized samples are listed in Table 1.

The first term in eq 6, (dE/dP)^1, describes the energy shift due to the change of crystal field strength with pressure. In a point ion model, the Dq is proportional to R^{-5}, where R represents the distance between Mn^{2+} ions and surrounding S ions.[20] Therefore, the first term of the equation can be written as

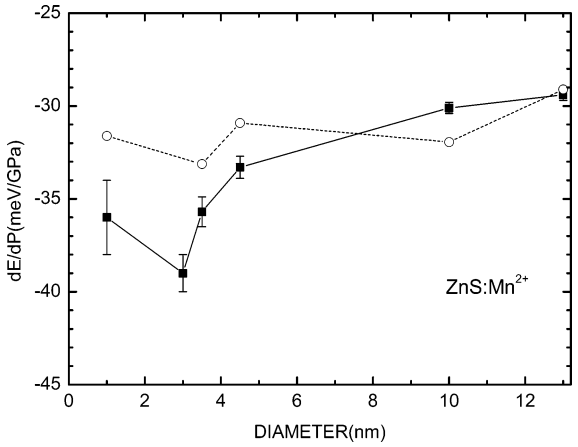

Figure 6. Variation of the pressure coefficient of the ZnS:Mn^{2+} nanoparticles as a function of the diameter of particle. ○ represents the evaluated values, and ■ represents the experimental data. The value of the bulk is also drawn on the right vertical axis of the figure for comparison.

$$\left(\frac{\mathrm{d}E}{\mathrm{d}P}\right)^1 = -10\frac{\mathrm{d}Dq}{\mathrm{d}P} = -\frac{50}{3}kDq \tag{12}$$

where $k = -1/V(\mathrm{d}V/\mathrm{d}P)$ is the volume compressibility of ZnS. The reported value of k for bulk ZnS is 1.27×10^{-2} Gpa^{-1}.[22] The second term in eq 6, (dE/dP)^2, depicts the contribution of covalence, which results from the variation of inner shell electron states of Mn^{2+} with pressure. The experimental value of dB/dP is -3.48 meV/GPa for bulk ZnS:Mn.[23] However, no data for k and dB/dP are available for ZnS:Mn^{2+} nanoparticles. We adapted the data for k and dB/dP of bulk ZnS:Mn^{2+} for the nanoparticle calculations by assuming that these two parameters are not size dependent. The calculated results of dE/dP are listed in Table 1 and shown in Figure 6 along with experimental data.

The calculated pressure coefficient of bulk ZnS:Mn^{2+} is -29.1 meV/GPa, which is very close to the observed value of -29.4 ± 0.3 meV/GPa. The pressure coefficients for nanosized samples calculated from eq 6 are also in agreement with the experimental data qualitatively. The theoretical results of the first and second terms in eq 6 for differently sized nanoparticles are also given in Table 1. The results indicate that the second term in eq 6 is much more important than the first term in determining the pressure coefficient—that is to say, the pressure coefficient is more sensitive to the Racah parameter B.

It is noted that the calculated results deviates little from the observed pressure coefficients. The calculation is based only on the crystal field theory while other effects such as phonon coupling and the interaction with surface states may also influence the luminescence behavior.[10,12] Chen et al.[11] have indicated that the electron−phonon coupling strength in nanoparticles is size dependent and will affect the emission energy of the Mn^{2+} in ZnS:Mn^{2+} nanoparticles. In a similar way, it

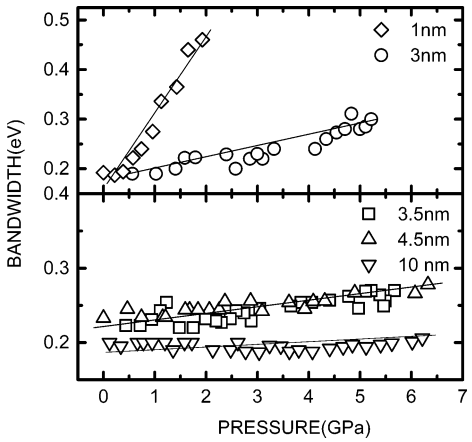

Figure 7. Pressure dependence of the emission bandwidth of Mn^{2+} in the 1-, 3-, 3.5-, 4.5-, and 10-nm-sized ZnS:Mn^{2+} nanoparticles. The solid lines serve only to guide the eye.

can affect the pressure behaviors. In addition, Mn^{2+} ions in ZnS:Mn^{2+} nanoparticles are distributed in the bulk sites and the near-surface sites. The Mn^{2+} ions at the near-surface sites have different site environments than the Mn^{2+} ions in the bulk ZnS lattice sites. In the calculation, these discrepancies are not considered. Thus, it is reasonable that there are some differences between the theoretical and the observed results. However, the theoretical results are fairly close to the observations. This suggests that crystal field theory is still the major parameter governing the pressure behaviors of the luminescence.

In addition to the emission energy and intensity, the pressure dependence of the emission bandwidth of Mn^{2+} in ZnS:Mn^{2+} nanoparticles is also size dependent. Figure 7 shows the pressure dependence of the bandwidth of differently sized particles. It is interesting to see that the bandwidth increase is faster with increasing pressure for smaller particles. The emission bandwidth increases slowly with increase of pressure for 10-, 4.5-, and 3.5-nm samples whereas the bandwidth increases significantly with increasing pressure for 3- and 1-nm particles. The emission bandwidth (W) at half-intensity can be related to the Huang−Rhys factor (S)[24,25] by

$$W = 4(\ln 2)^{1/2}(KTS\hbar\omega_{LO})^{1/2} \qquad (13)$$

where K is the Boltzmann constant, ω_{LO} is the LO-phonon frequency, T is the temperature, and $\hbar$ is Planck's constant. This means that the emission bandwidth is mainly determined by electron−phonon coupling and the LO-phonon frequency. The S values estimated from Stokes shifts for 1-, 3.5-, 4.5-, and 10-nm particles and bulk ZnS:Mn^{2+} are 2.41, 2.88, 3.18, 3.33, and 3.09, respectively.[11] These results indicate that phonon coupling is not responsible for the size dependence of bandwidth on pressure. On the other hand, it was reported that the LO-phonon frequency of nanoparticles is higher than the bulk,[26] such as for bulk ZnS:Mn, $\hbar\omega_{LO} = 350$ cm^{-1},[27] and for 3.6-nm nanoparticles, $\hbar\omega_{LO} = 423$ cm^{-1}.[26] The increase of phonon frequency is perhaps one of the reason for the faster increase of the bandwidth with increasing pressure for smaller particles. Furthermore, the average S value for Mn^{2+} obtained from the emission bandwidths is larger than that obtained from the Stokes shift of Mn^{2+} nanoparticle emission from the lowest excited state (∼2.88).[11,12] This means that there exists possibly other broadening mechanisms in addition to the electron−phonon interaction.[12] This additional broadening may result from either a distribution of particle sizes or a distribution of Mn^{2+} environments. Electron spin resonance (ESR) studies have demonstrated that more Mn^{2+} ions are at the near-surface sites for smaller particles.[11] Mn^{2+} ions at the near-surface sites have an axial lower crystal field than Mn^{2+} ions at the lattice sites.[2] The axial or lower crystal fields may relax the transition selection rules and accelerate recombination for the enhancement of luminescence.[2] Mn^{2+} ions at the near-surface sites may experience pressure change more effectively than Mn^{2+} ions at the lattice sites. This may cause a larger increase in the emission bandwidth with increasing pressure for smaller sized nanoparticles.

Conclusion

In summary, the pressure behavior of Mn^{2+} emission in differently sized ZnS:Mn^{2+} nanoparticles is investigated. The emission shifts to lower energies with increasing pressure and the shift rate (the absolute value of the pressure coefficient) is larger in the ZnS:Mn^{2+} nanoparticles than in bulk. The pressure coefficient increases with the decrease of the particle size with the 1-nm-sized particles as an exception. The pressure coefficients calculated on the basis of the crystal field theory are in agreement with the experimental results. It is also observed that, for particles with average sizes of 3.5, 4.5, and 10 nm and bulk ZnS:Mn^{2+}, the luminescence intensity of Mn^{2+} is weakly dependent on pressure, while, for particles 1 and 3 nm in size, the luminescence intensity of Mn^{2+} is quenched dramatically at increasing pressure. The bandwidth increase is faster with increasing pressure for smaller particles. This is attributed to the fact that more Mn^{2+} ions are at the near-surface sites and because of the increase of the phonon frequency for smaller nanoparticles. These new observations are helpful for understanding the luminescence mechanisms in doped nanoparticles.

Acknowledgment. This work was partly supported by the National Natural Science Foundation of China (Contract No. 60076012) and the Nanometer Science and Technology Program of the Chinese Academy of Sciences. W.C. thanks Nomadics, Inc., the National Science Foundation (Grant DMI-0132030), and the Air Force Office of Scientific Research (Contract No. F49620-00-C-0058) for financial support. Bob Hilley is acknowledged for critically reading the manuscript.

References and Notes

(1) Wang, Y.; Herron, N. *J. Phys. Chem.* **1991**, *95*, 525 and references therein.
(2) Bhargava, R. N.; Gallagher, D.; Hong, X.; Nurmikko, A. *Phys. Rev. Lett.* **1994**, *72*, 416.
(3) Bol, A. A.; Meijerink, A. *Phys. Rev. B.* **1998**, *58*, R15997.
(4) Smith, B. A.; Zhang, J. Z.; Joly, A.; Liu, J. *Phys. Rev. B* **2000**, *62* (3), 2021.
(5) Murase, N.; Jagannathan, R.; Kanematsu, Y.; Watanabe, M.; Kurita, A.; Hirata, K.; Yazawa, T.; Kushida, T. *J. Phys. Chem. B* **1999**, *103* (5), 754.
(6) Chung, J. H.; Ah, C. S.; Jang, D.-J. *J. Phys. Chem. B* **2001**, *105*, 4128.
(7) Godlewski, M.; Ivanov, V. Yu.; Bergman, P. J.; Monemar, B.; Golacki, Z.; Karczewski, G. *J. Alloys. Compd.* **2002**, *341*, 8.
(8) Yu, J.; Liu, H.; Wang, Y.; Jia, W. *J. Lumin.* **1998**, *79*, 191.
(9) de Mello Donegá, C.; Bol, A. A.; Meijerink, A. *J. Lumin.* **2002**, *96*, 87.
(10) Chen, W.; Li, G. H.; Malm, J.-O.; Huang, Y.; Wallenberg, R. *J. Lumin.* **2000**, *91*, 139.
(11) Chen, W.; Sammynaiken, R.; Huang, Y.; Malm, J.-O.; Wallenberg, R.; Bovin, J.-O.; Zwiller, V.; Kotov, N. A. *J. Appl. Phys.* **2001**, *89*, 1120. Chen, W.; Sammynaiken, R.; Huang, Y. *J. Appl. Phys.* **2000**, *88*, 5188.
(12) Chen, W.; Su, F. H.; and Li, G. H.; Joly, A. G.; Malm, J.-O.; Bovin, J.-O. *J. Appl. Phys.* **2002**, *92*, 1950.
(13) Chen W., Wang Z. G., Lin Z. J.; Lin L. Y. *J. Mater. Sci. Technol.* **1997**, *13*, 397.

(14) Kezuka, T.; Konishi, T.; Isobe, T.; Senna, M. *J. Lumin.* **2000**, *87*−*89*, 418. Kubo, T.; Isobe, T.; Senna, M. *J. Lumin.* **2002**, *99*, 39.
(15) Joly, A. G.; Chen, W.; Roark, J.; Zhang, J. Z. *J. Nanosci. Nanotechnol.* **2001**, *1*, 295.
(16) Chen, W.; Joly, A. G.; Roark, J. *Phys. Rev. B* **2002**, *65*, 2454041−8.
(17) Ozin, G. A. *Adv. Mater.* **1992**, *4*, 612.
(18) House, G. L.; Drickamer, H. G. *J. Chem. Phys.* **1997**, *67*, 3230.
(19) Tanabe, Y.; Sugano, S. *J. Phys. Soc. Jpn.* **1954**, *9*, 753.
(20) Ves, S.; Strossner, K.; Gebhardt, W.; Cardona, M. *Phys. Rev. B* **1986**, *33*, 4077.
(21) Ford, R. A.; Kauer, E.; Rabenau, A.; Brown, D. A. *Ber. Bunsen-Ges. Phys. Chem.* **1962**, *67*, 460.
(22) Montalva, R. A.; Langer, D. W. *J. Appl. Phys.* **1970**, *41*, 4101.
(23) Koda, T.; Shionoya, S.; Ichikawa, M. *J. Phys. Chem. Solids* **1966**, *27*, 1577.
(24) Huang, K.; Rhys, A. *Proc. R. Soc. London, Ser. A* **1950**, *204*, 406.
(25) Huang, K. *Prog. Phys.* **1981**, *1*, 31 (in Chinese).
(26) Yu, J. Q.; Liu, H. M.; Wang, Y. Y.; Fernandez, F. E.; Jia, W. Y. *J. Lumin.* **1998**, *76 & 77*, 252.
(27) Anastassiadou, A.; Liarocapis, E.; Anastassakis, E. *Solid State Commun.* **1988**, *69*, 137.